per sample area) were measured as dependent variable and treatment means, sample sizes and variance estimates were reported. Included were two experiments on macroalgae (this study), five experiments with periphyton in freshwater, brackish and marine ecosystems[27,28], two experiments with salt marsh plants[29], and one with lake phytoplankton[30], including subtropical and temperate climates in North America and Europe. We analysed data from sampling dates when species richness reached the seasonal peak, which was usually in late spring or summer. Data were standardized using the common meta-analysis metric of standardized effect size, Hedges's *d* (ref. 21). This is a measure of the difference between experimental and control means, divided by a pooled standard deviation and multiplied by a correction factor to account for small sample sizes. Homogeneity of effect sizes was tested using the *Q*-statistic[21]. As we detected significant heterogeneity among effect sizes we split the data set into low-productivity (oligotrophic and mesotrophic) and high-productivity (eutrophic) sites, based on information provided in the publications.

Received 23 January; accepted 12 April 2002; doi:10.1038/nature00830.

1. Hutchinson, G. E. Homage to Santa Rosalia, or why are there so many kinds of animals. *Am. Nat.* **93,** 145–159 (1959).
2. Tilman, D. Causes, consequences and ethics of biodiversity. *Nature* **405,** 208–211 (2000).
3. Sommer, U. & Worm, B. (eds) *Competition and Coexistence* (Springer, Berlin, 2002).
4. Connell, J. H. Diversity in tropical rain forests and coral reefs. *Science* **199,** 1302–1310 (1978).
5. Tilman, D. *Resource Competition and Community Structure* (Princeton Univ. Press, Princeton, 1982).
6. Flöder, S. & Sommer, U. Diversity in planktonic communities: an experimental test of the intermediate disturbance hypothesis. *Limnol. Oceanogr.* **44,** 1114–1119 (1999).
7. Buckling, A., Kassen, R., Bell, G. & Rainey, P. B. Disturbance and diversity in experimental microcosms. *Nature* **408,** 961–964 (2000).
8. Kassen, R., Buckling, A., Bell, G. & Rainey, P. B. Diversity peaks at intermediate productivity in laboratory microcosms. *Nature* **406,** 508–512 (2000).
9. Huston, M. A. *Biological Diversity* (Cambridge Univ. Press, Cambridge, 1994).
10. Kondoh, M. Unifying the relationships of species richness to productivity and disturbance. *Proc. R. Soc. Lond. B* **268,** 269–271 (2001).
11. Vitousek, P. M. *et al.* Human alteration of the global nitrogen cycle: sources and consequences. *Ecol. Appl.* **7,** 737–750 (1997).
12. Pauly, D., Christensen, V., Dalsgaard, J., Froese, R. & Torres, F. Jr Fishing down marine food webs. *Science* **279,** 860–863 (1998).
13. Jackson, J. B. C. *et al.* Historical overfishing and the recent collapse of coastal ecosystems. *Science* **293,** 629–638 (2001).
14. Tilman, D. Competition and biodiversity in spatially structured habitats. *Ecology* **75,** 2–16 (1994).
15. Mann, K. H. Seaweeds: their productivity and strategy for growth. *Science* **182,** 975–981 (1973).
16. Nielsen, K. J. Bottom-up and top-down forces in tide pools: test of a food chain model in an intertidal community. *Ecol. Monogr.* **71,** 187–217 (2001).
17. Menge, B. A. & Sutherland, J. P. Community regulation: variation in disturbance, competition, and predation in relation to environmental stress and recruitment. *Am. Nat.* **130,** 730–757 (1987).
18. Sorokin, Y. I. *Coral Reef Ecology* (Springer, Berlin, 1995).
19. Worm, B., Lotze, H. K. & Sommer, U. Coastal food web structure, carbon storage and nitrogen retention regulated by consumer pressure and nutrient loading. *Limnol. Oceanogr.* **45,** 339–349 (2000).
20. Chapin, F. S. III *et al.* Consequences of changing biodiversity. *Nature* **405,** 234–242 (2000).
21. Gurevitch, J., Morrison, J. A. & Hedges, L. V. The interaction between competition and predation: a meta-analysis of field experiments. *Am. Nat.* **155,** 435–453 (2000).
22. Terborgh, J. *et al.* Ecological meltdown in predator-free forest fragments. *Science* **294,** 1923–1925 (2001).
23. Watling, L. & Norse, E. A. Disturbance of the seabed by mobile fishing gear: a comparison to forest clearcutting. *Conserv. Biol.* **12,** 1180–1197 (1998).
24. Lotze, H. K., Worm, B. & Sommer, U. Strong bottom-up and top-down control of early life stages of macroalgae. *Limnol. Oceanogr.* **46,** 749–757 (2001).
25. Worm, B., Reusch, T. B. H. & Lotze, H. K. *In situ* nutrient enrichment: methods for marine benthic ecology. *Internat. Rev. Hydrobiol.* **85,** 359–375 (2000).
26. Stirling, G. & Wilsey, B. Empirical relationships between species richness, evenness, and proportional diversity. *Am. Nat.* **158,** 286–299 (2001).
27. Hillebrand, H., Worm, B. & Lotze, H. K. Marine microbenthic community structure regulated by nitrogen loading and herbivore pressure. *Mar. Ecol. Prog. Ser.* **204,** 27–38 (2000).
28. Hillebrand, H. & Kahlert, M. Effect of grazing and nutrient supply on periphyton biomass and nutrient stoichiometry in habitats of different productivity. *Limnol. Oceanogr.* **46,** 1881–1898 (2001).
29. Gough, L. & Grace, J. B. Herbivore effects on plant species density at varying productivity levels. *Ecology* **79,** 1586–1594 (1998).
30. Proulx, M., Pick, F. R., Mazumder, A., Hamilton, P. B. & Lean, D. R. S. Experimental evidence for interactive impacts of human activities on lake algal species richness. *Oikos* **76,** 191–195 (1996).

Acknowledgements

We thank L. Gough, R. Karez, D. Kehler, I. Milewski, R. A. Myers, R. T. Paine and T. B. H. Reusch for comments, and J. Gurevitch for statistical advice. This work was funded by the German Research Council (DFG) and the German Ministry of Science and Education.

Competing interests statement

The authors declare that they have no competing financial interests.

Correspondence and requests for materials should be addressed to B.W. (e-mail: bworm@is.dal.ca).

A global analysis of *Caenorhabditis elegans* operons

Thomas Blumenthal*, Donald Evans*, Christopher D. Link†, Alessandro Guffanti‡, Daniel Lawson‡, Jean Thierry-Mieg§, Danielle Thierry-Mieg§, Wei Lu Chiu‖, Kyle Duke¶, Moni Kiraly¶ & Stuart K. Kim¶

* *Department of Biochemistry and Molecular Genetics, University of Colorado School of Medicine, Box B121, 4200 E. 9th Avenue, Denver, Colorado 80262, USA*
† *Institute of Behavioral Genetics, Box 447, University of Colorado, Boulder, Colorado 80309, USA*
‡ *The Sanger Centre, Wellcome Trust Genome Campus, Hinxton, Cambridge CB10 1SA, UK*
§ *Gene Network Laboratory, National Institute of Genetics, Mishima 411, Japan, and National Center for Biotechnology Information, Bethesda, Maryland, USA*
‖ *Department of Molecular Sciences and Technologies, Pfizer Global Research & Development—Ann Arbor, 2800 Plymouth Road, Ann Arbor, Michigan 48105, USA*
¶ *Departments of Developmental Biology and Genetics, Stanford University Medical Center, 279 Campus Drive, Stanford, California 94305, USA*

The nematode worm *Caenorhabditis elegans* and its relatives are unique among animals in having operons[1]. Operons are regulated multigene transcription units, in which polycistronic pre-messenger RNA (pre-mRNA coding for multiple peptides) is processed to monocistronic mRNAs. This occurs by 3′ end formation and *trans*-splicing using the specialized SL2 small nuclear ribonucleoprotein particle[2] for downstream mRNAs[1]. Previously, the correlation between downstream location in an operon and SL2 *trans*-splicing has been strong, but anecdotal[3]. Although only 28 operons have been reported, the complete sequence of the *C. elegans* genome reveals numerous gene clusters[4]. To determine how many of these clusters represent operons, we probed full-genome microarrays for SL2-containing mRNAs. We found significant enrichment for about 1,200 genes, including most of a group of several hundred genes represented by complementary DNAs that contain SL2 sequence. Analysis of their genomic arrangements indicates that >90% are downstream genes, falling in 790 distinct operons. Our evidence indicates that the genome contains at least 1,000 operons, 2–8 genes long, that contain about 15% of all *C. elegans* genes. Numerous examples of co-transcription of genes encoding functionally related proteins are evident. Inspection of the operon list should reveal previously unknown functional relationships.

In order to search the genome for mRNAs that contain SL2, we hybridized microarrays containing 17,817 predicted genes (94% of known and predicted genes) with probe enriched for SL2-containing mRNAs (see Methods). The results are presented in Fig. 1a. The line shows that the genes form three peaks, a peak of about 1,200 genes with very high SL2/poly(A)$^+$ ratios and two larger peaks with low SL2/poly(A)$^+$ ratios containing the remainder of the genes. As a positive control, we identified 319 genes that produce SL2-containing mRNAs on the basis of analysis of the sequence traces of cDNAs from the Y. Kohara laboratory (listed in Supplementary Information Table 1). Fig. 1a shows that most (84%) of these were among the SL2-enriched genes. Negative controls include 100 genes that are the first genes in the operons identified by the 100 highest SL2/poly(A)$^+$ scores, and very few of these are among the SL2-enriched genes (Fig. 1b). We conclude that the microarray probing successfully identified genes that are *trans*-spliced to SL2.

Having performed a global search for genes that produce SL2 mRNAs, we determined whether their genomic structure indicated that they are located within operons. Each gene was evaluated as to whether it was likely to be downstream in an operon by the criteria described in Fig. 1 legend, using either the WormBase[5] or the

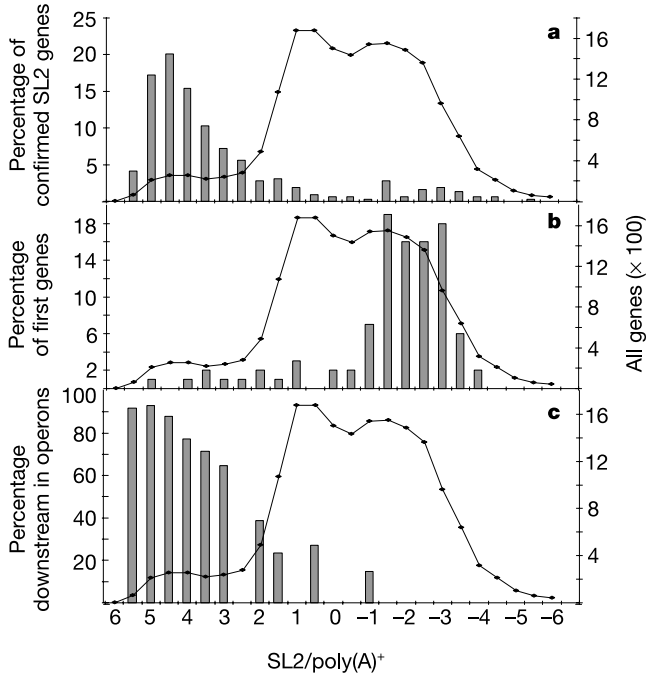

Figure 1 SL2/poly(A)$^+$ ratios of 17,817 *C. elegans* genes. Genes were divided into bins according to ratios, and plotted as $\log_2$(ratio) (line). **a**, Distribution of confirmed SL2-accepting genes. Percentage of 319 genes shown to be SL2 *trans*-spliced on the basis of sequenced cDNAs (bars). **b**, Distribution of first genes in operons. First genes in the operons identified by the 100 highest SL2/poly(A)$^+$ ratios were distributed into bins. **c**, Genes in the leftmost peak and four control groups of 100 genes were evaluated for location in operons. Genes whose *trans*-splice sites were within 1 kb of the stop codon or 500 bp from the poly(A) site of another gene were scored as downstream in operons. Percentage of genes in each bin scored as downstream in operons is shown.

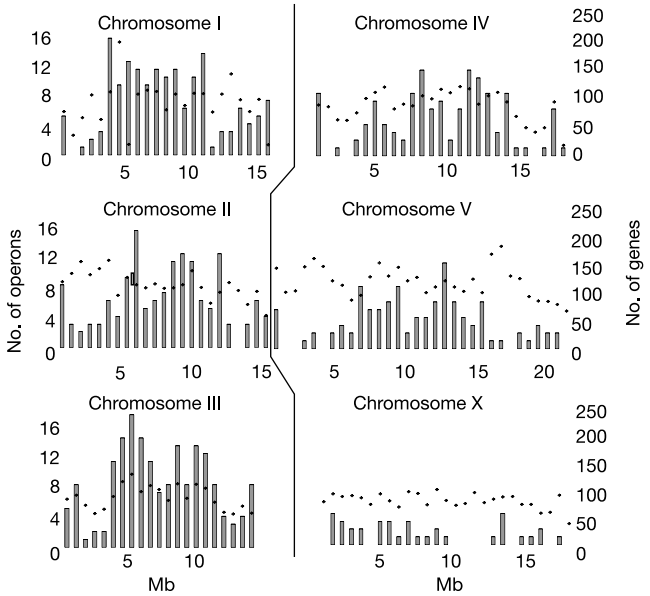

Figure 2 Chromosomal distribution of operons. Each chromosome was divided into equal-sized bins of 665,230 bp. The *x* axis is in Mb from the left end of each chromosome. The number of predicted genes in each bin (right-hand *y* axis) is shown by the data points. Operons (left-hand *y* axis) are shown as bars.

Intronerator website[6]. In the set of 1,200 SL2-enriched genes contained in the leftmost peak, 86% were scored as downstream in operons, and only 4.5% were scored as first genes in operons (Fig. 1c). From the set of genes that do not show significant SL2/poly(A)$^+$ ratios, only 15–20% were scored as possibly downstream in operons. This analysis provides strong evidence that the microarray experiment effectively identified *C. elegans* genes that are in operons. These data show a robust correlation across the genome between SL2 *trans*-splicing and downstream location in an operon, confirming and extending previous data based on individual genes.

We used three methods to estimate the number of operons in the genome. First, we collected all of the genes in operons, both from microarray data and in the list of SL2-containing cDNAs. The combined list contains 2,291 genes in 881 operons (Supplementary Information Table 2). Second, we estimated the number of operons that were missed by the microarray data. The list of SL2 spliced genes identified in the microarray experiments contained 74% of the genes identified from cDNA clones, and thus presumably of all SL2 spliced genes. Therefore we estimate that the genome contains at least 1,068 operons (790/0.74). Third, genes can be predicted to be in operons on the basis of their gene structure. We formed a list of possible operons on the basis of gene orientation and a spacing of less than 1 kilobase (kb) between stop and start codons. There are >3,000 possible operons on this list, and 790 of these were found to be SL2-enriched in our microarray experiments. On average, the remaining genes express transcripts that are at comparable levels to the SL2-containing transcripts, making it unlikely that we missed many genes because they are expressed at too low a level to have been detected on the microarrays or by cDNA clones. Instead, the remaining genes may not be in operons, but instead may be genes that are fortuitously close together.

The average operon contains 2.6 genes, and the longest contains 8 genes (Table 1). 332 operons have more than two genes, and in 58% of these every downstream gene was scored as SL2 *trans*-spliced. These data indicate that a large percentage of SL2-accepting genes were identified, and provide strong support for the conclusion that downstream genes in operons are usually or always *trans*-spliced by SL2. If there are about 1,000 operons with 2.6 genes per operon, there are ~2,600 genes in operons. Thus the *C. elegans* genome, which contains between 17,300 (estimated from expressed open reading frames[7]) and 19,000 (all known and predicted open reading frames[5]) genes, expresses at least 13–15% of its genes as operons.

Table 1 The number of genes per operon

Genes per operon	No. of operons
2	549
3	207
4	75
5	33
6	13
7	3
8	1

Table 2 Operons containing human disease gene orthologues

Gene	Disease	No. of genes in operon
B0261.2	Ataxia telangiectasia (ATM)	3
C01G8.5	Neurofibromatosis, type 2/Batten's disease	4
C15F1.7	Amyotrophic lateral sclerosis (ALS)	3
C16C2.3	Lowe syndrome	3
C48E7.4	Primary open angle glaucoma	4
F12F6.3	Hereditary multiple exostoses	2
F53H8.1	Hermansky–Pudlak syndrome	2
F59G1.7	Friedreich ataxia (FRDA)	7
K08E3.7	Parkinson's disease, juvenile 2	2
Y110A7A.5	Myotubular myopathy	5
Y56A3A.13	Fragile hystidine triad	3
Y76A2A.2	Menkes syndrome/Wilson disease	5
ZK675.1	Nevoid basal cell carcinoma syndrome	2

An expanded version of this list, containing hypothesized functions for all of the genes in the operons, can be found in Supplementary Information.

These operons are not evenly distributed on the *C. elegans* chromosomes (Fig. 2). The X chromosome has only 37 identified operons (2.1 per megabase, Mb), whereas chromosome III has 207 (16.2 per Mb). The availability of thousands of cDNA clones allowed estimation of the distance between genes for 285 operon gene pairs (Fig. 3). The mean intercistronic distance is 126-base pairs (bp), with most between 100 and 120 bp.

The correlation between SL2 *trans*-splicing and downstream position in an operon is quite strong. Nonetheless some genes that appear to be downstream in operons do not have high SL2/poly(A)$^+$ scores, perhaps because their mRNAs were not well represented in the probe RNA population. Some operons that are expressed at low levels may have been missed. Also, some downstream genes in operons may get *trans*-spliced to SL1 rather than SL2[8]. Operons with long spacing might be missed because they have a tendency to be SL1 spliced[3]. Furthermore, some genes that do get SL2 *trans*-spliced appear not to be downstream in operons. Perhaps there is a rare mode of SL2 *trans*-splicing that does not require a gene to be downstream in an operon.

Operons are a common form of gene organization in bacteria and archaea, but they are in general absent in eukaryotes (with the possible exception of trypanosomes). Based on genome sequences of yeast, *Arabidopsis*, *Drosophila* and humans, operons are very unlikely to be found in this wide array of species. *Trans*-splicing appears to be an enabling characteristic. Presumably operons exist only when *trans*-splicing can provide a cap to protect the downstream RNA following 3′ end cleavage and prevent the accompanying transcription termination. Operons have been reported only in rhabditid nematodes[9], although recent work suggests they are found elsewhere among the nematodes (D. G. Giliano and M. Blaxter, personal communication). Nevertheless, the fact that operon organization in *C. elegans* is so common implies that the genome may be quite plastic, perhaps owing to chromosomal rearrangements producing new gene juxtapositions[10]. Given the relatively compact *C. elegans* genome, operon evolution may have been driven in part by constraints on chromosomal structure or organization.

Caenorhabditis elegans operons appear to be a means to co-regulate functionally related proteins, like bacterial operons. Related genes do occur in operons[11–15]. Indeed, numerous additional examples are found in the list of operons reported here. For example, *D1054.2*, encoding a proteasome subunit, is in an operon with a ubiquitin ligase complex subunit. *ZK856.9*, which encodes a TFIIIC transcription factor, is in an operon with an RNA polymerase III subunit. *C15H11.9*, encoding a regulator of ribosome synthesis, is in an operon with an RNA polymerase I subunit. *C15C7.1*, encoding a vesicle docking and trafficking protein, is in an operon with a GRIP domain protein that also functions in the *trans*-Golgi. These and numerous other examples show that related genes are often found together in operons. Furthermore, such relationships occur far more frequently than would be expected by chance. For example, all seven genes with an RNA-binding domain of the 'RNA recognition motif' (RRM) type that are in operons with other genes with identified functions are in operons with other nucleic-acid-interacting proteins. In contrast, of seven proteins likely to be involved with the Golgi, only one operon contains a nucleic-acid-binding protein, whereas four contain proteins related to transport. Our results show that genes for mitochondrial proteins have a strong tendency to be in operons with genes for other mitochondrial proteins, and that this relationship is highly significant ($P = 3.6 \times 10^{-4}$; see Supplementary Information Tables 3 and 4). The same is true for genes encoding splicing proteins. However, whether operons usually contain genes of related function is not yet known.

Nonetheless, the presence of a gene in an operon with another gene has recently been used to successfully predict a previously unknown functional relationship[16], suggesting that the operons can be used to uncover related genes. We note that many examples of genes in operons are apparent orthologues of genes that cause disease in humans[17] (Table 2). It may be possible to identify novel genes that are functionally related to the disease genes by investigating the other genes in these operons. □

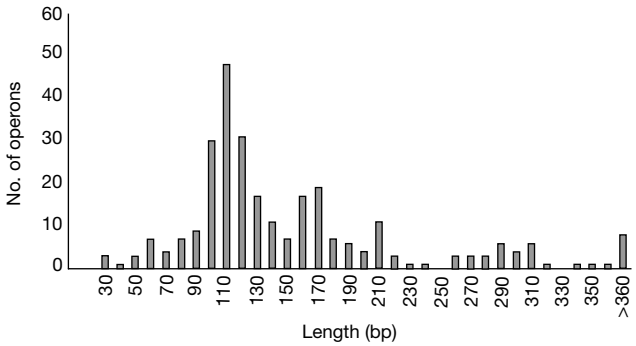

Figure 3 Operon intercistronic distances. Distances from the 3′ end formation site of upstream genes and *trans*-splice sites of downstream genes are plotted for the 285 operons for which reliable data are available (listed in Supplementary Information Table 6).

Methods

SL2-enriched cDNA was prepared by reverse transcribing 5 μg of mixed stage poly(A)$^+$ RNA primed with oligo(dT)[18]. The cDNA was denatured at 70 °C for 2 min, and annealed to a T7/SL2 primer (1 μM; 5′-TGAATTGTAATACGACTCACTATAGGGAGA GGTTTTAACCCAGTTACTCA-3′) at 42 °C for 5 min, followed by extension with *Escherichia coli* DNA polymerase I Klenow fragment in 100 μl at 37 °C for 30 min. RNase H was destroyed by incubating with 0.5% SDS and 20 μg proteinase K for 1 h at 55 °C. The cDNA was extracted with phenol, phenol/chloroform, chloroform/isoamyl alcohol and ethanol precipitated. SL2-enriched cRNA was prepared using T7 RNA polymerase using the manufacturer's Megascript protocol (Ambion). DNA microarrays are described in ref. 19. RNA preparation, cDNA synthesis, labelled cDNA preparation, microarray hybridization and microarray scanning were performed as previously described[18]. Cy3-dUTP was used to label SL2-enriched cDNA and Cy5-dUTP was used to label cDNA from poly(A)$^+$ RNA made from a mixed stage population of wild-type worms. The SL2-enriched probe and the probe from the starting poly(A)$^+$ mRNA were simultaneously hybridized to DNA microarrays. To ensure reproducibility, this procedure was repeated five times. Ratios of Cy3/Cy5 (SL2/poly(A)$^+$) signals were calculated for each gene and converted to $\log_2$(ratio). We then calculated the average $\log_2$(ratio) from the five repeats. The full data set is available as Supplementary Information Table 5. The results are presented by dividing the resulting $\log_2$(ratios) into bins (Fig. 1a).

Received 9 November 2001; accepted 15 April 2002; doi:10.1038/nature00831.

1. Spieth, J., Brooke, G., Kuersten, S., Lea, K. & Blumenthal, T. Operons in *C. elegans*: Polycistronic mRNA precursors are processed by trans-splicing of SL2 to downstream coding regions. *Cell* **73,** 521–532 (1993).
2. Huang, X.-Y. & Hirsh, D. A second trans-spliced RNA leader sequence in the nematode *Caenorhabditis elegans*. *Proc. Natl Acad. Sci. USA* **86,** 8640–8644 (1989).
3. Blumenthal, T. & Steward, K. in *C. Elegans II* (eds D. L. Riddle *et al.*) 117–145 (Cold Spring Harbor Laboratory Press, Cold Spring Harbor, 1997).
4. Zorio, D. A. R., Cheng, N., Blumenthal, T. & Spieth, J. Operons represent a common form of chromosomal organization in *C. elegans*. *Nature* **372,** 270–272 (1994).
5. Stein, L., Sternberg, P., Durbin, R., Thierry-Mieg, J. & Spieth, J. WormBase: network access to the genome and biology of *Caenorhabditis elegans*. *Nucleic Acids Res.* **29,** 82–86 (2001).
6. Kent, W. J. & Zahler, A. M. The intronerator: exploring introns and alternative splicing in *Caenorhabditis elegans*. *Nucleic Acids Res.* **28,** 91–93 (2000).
7. Raboul, J. *et al.* Open-reading-frame sequence tags (OSTs) support the existence of at least 17,300 genes in *C. elegans*. *Nature Genet.* **27,** 332–336 (2000).
8. Williams, C., Xu, L. & Blumenthal, T. SL1 trans-splicing and 3′ end formation in a unique class of *Caenorhabditis elegans* operon. *Mol. Cell. Biol.* **19,** 376–383 (1999).
9. Evans, D. *et al.* Operons and SL2 trans-splicing exist in nematodes outside the genus *Caenorhabditis*. *Proc. Natl. Acad. Sci. USA* **94,** 9751–9756 (1997).
10. Huynen, M. A., Snel, B. & Bork, P. Inversions and the dynamics of eukaryotic gene order. *Trends Genet.* **17,** 304–306 (2001).
11. Page, A. P. Cyclophilin and protein disulphide isomerase genes are co-transcribed in a functionally related manner in *Caenorhabditis elegans*. *DNA Cell Biol.* **16,** 1335–1343 (1997).
12. Huang, L. S., Tzou, P. & Sternberg, P. W. The *lin-15* locus encodes two negative regulators of *Caenorhabditis elegans* vulval development. *Mol. Biol. Cell* **5,** 395–412 (1994).
13. Clark, S. G., Lu, X. & Horvitz, H. R. The *Caenorhabditis elegans* locus *lin-15*, a negative regulator of a tyrosine kinase signalling pathway, encodes two different proteins. *Genetics* **137,** 987–997 (1994).
14. Treinin, M., Gillo, B., Liebman, L. & Chalfie, M. Two functionally dependent acetylcholine subunits are encoded in a single *Caenorhabditis elegans* operon. *Proc. Natl Acad. Sci. USA* **95,** 15492–15495 (1998).
15. Mazroui, R., Puoti, A. & Kramer, A. Splicing factor SF1 from *Drosophila* and *Caenorhabditis*: presence of an N-terminal RS domain and requirement for viability. *RNA* **5,** 1615–1631 (1999).

16. Furst, J. *et al.* ICln ion channel splice variants in *Caenorhabditis elegans*. Voltage dependence and interaction with an operon partner protein. *J. Biol. Chem.* **277,** 4435–4445 (2002).
17. Culetto, E. & Sattelle, D. B. A role for *Caenorhabditis elegans* in understanding the function and interactions of human disease genes. *Hum. Mol. Genet.* **9,** 869–877 (2000).
18. Reinke, V. *et al.* A global profile of germline gene expression in *C. elegans*. *Mol. Cell* **6,** 605–616 (2000).
19. Jiang, M. *et al.* Genome-wide analysis of developmental and sex-regulated gene expression profiles in *Caenorhabditis elegans*. *Proc. Natl Acad. Sci. USA* **98,** 218–223 (2001).

Supplementary Information accompanies the paper on *Nature*'s website (http://www.nature.com/nature).

Acknowledgements

We thank J. Spieth, J. Kent, A. Zahler and L. Stein for help with navigation of the *C. elegans* databases, Y. Kohara for cDNA data, M. Huang for discussions, I. Shah for statistical advice, D. Guiliano and M. Blaxter for communication of unpublished results, and P. MacMorris for advice on the manuscript. This work was supported by the NIH (T.B., C.D.L. and S.K.K.).

Competing interests statement

The authors declare that they have no competing financial interests.

Correspondence and requests for materials should be addressed to T.B. (e-mail: tom.blumenthal@uchsc.edu).

Feedback inhibition controls spike transfer in hybrid thalamic circuits

Gwendal Le Masson*, Sylvie Renaud-Le Masson†, Damien Debay‡ & Thierry Bal‡

** Laboratoire de Physiopathologie des Réseaux Neuronaux Médullaires, EPI INSERM 9914, Institut François Magendie, Université Victor Segalen Bordeaux 2, 1 Rue Camille Saint Saëns, 33077 Bordeaux Cedex, France*
† Laboratoire IXL, CNRS UMR 5818, ENSEIRB, Université de Bordeaux 1, 351 Cours de la Libération, 33405 Talence Cedex, France
‡ Unité de Neurosciences Intégratives et Computationnelles, CNRS UPR 2191, Institut de Neurobiologie Alfred Fessard, 1 Avenue de la Terrasse, 91198 Gif-sur-Yvette Cedex, France

Sensory information reaches the cerebral cortex through the thalamus, which differentially relays this input depending on the state of arousal[1–5]. Such 'gating' involves inhibition of the thalamocortical relay neurons by the reticular nucleus of the thalamus[6–8], but the underlying mechanisms are poorly understood. We reconstructed the thalamocortical circuit as an artificial and biological hybrid network *in vitro*. With visual input simulated as retinal cell activity, we show here that when the gain in the thalamic inhibitory feedback loop is greater than a critical value, the circuit tends towards oscillations—and thus imposes a temporal decorrelation of retinal cell input and thalamic relay output. This results in the functional disconnection of the cortex from the sensory drive, a feature typical of sleep states. Conversely, low gain in the feedback inhibition and the action of noradrenaline, a known modulator of arousal[4,9,10], converge to increase input–output correlation in relay neurons. Combining gain control of feedback inhibition and modulation of membrane excitability thus enables thalamic circuits to finely tune the gating of spike transmission from sensory organs to the cortex.

The thalamus is the major gateway for the flow of sensory information to the cerebral cortex. Far from being a passive relay, this structure actively processes information before cortical integration. It is the first stage at which sensory signals can be gated during selective attention or during the transition from general arousal to sleep[1–5,8]. Although much is known about the anatomy and the synaptic and cellular properties of the thalamic networks, the nature of the sensory information processing throughout selective arousal and sleep–wake stages is not yet understood. The goal of this work was to investigate the mechanisms responsible for changes in the efficiency of sensory spike transfer in the retinothalamic network, during different states of arousal. We used hybrid biological–neuromimetic networks that allow direct control of cellular and synaptic components[11]. We measured the variations of spike-to-spike correlation between identified input and output neurons, reflecting the efficiency and reliability of signal transfer in different activity states.

In our hybrid networks (Fig. 1a), synaptic-like interactions between realistic conductance-based model neurons and an intracellularly recorded biological neuron run in real time, following the natural dynamics of the biological cell or network. Individual membrane currents of the simulated and biological neurons and the properties of their synaptic connections can be selectively and quantitatively controlled throughout their dynamic range, *in vitro* or *in vivo*. The required speed of real-time computation is achieved by using both programmable digital signal processors (DSPs) and newly designed analog integrated circuits[11,12]. A dynamic clamp procedure was used to simulate synaptic conductances by current injection through the intracellular recording pipette[13].

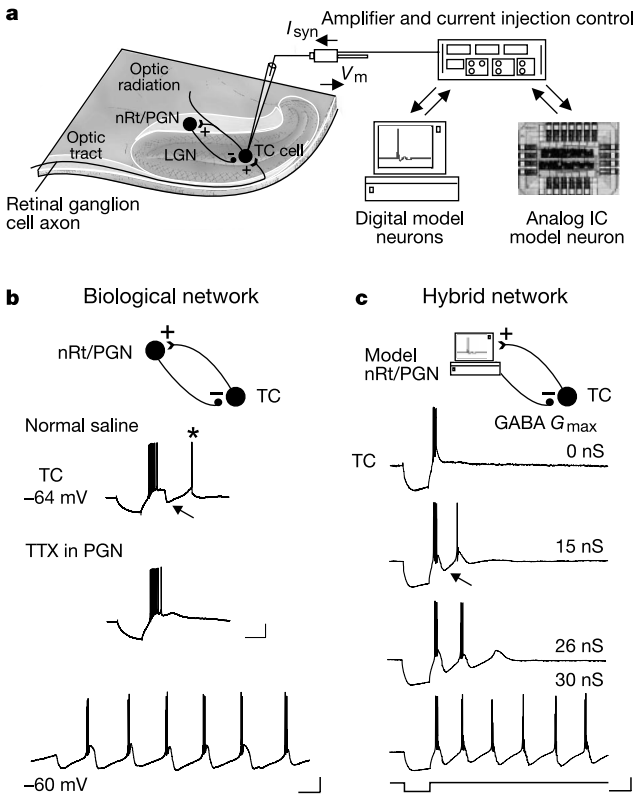

Figure 1 Design of hybrid thalamic circuits. **a**, Artificial synaptic connections between a biological TC cell recorded intracellularly in an LGNd slice and DSP-based and analog integrated circuit (IC) neurons. Wiring diagram in a ferret LGNd slice: +, excitatory; −, inhibitory. **b**, One-to-one coupling in ferret networks: a burst of spikes evoked in a single TC neuron can trigger burst firing of a target PGN neuron (not shown), which generates feedback inhibition[14–16] (arrow) and rebound burst (asterisk). Middle, tetrodotoxin (TTX) block of PGN activity prevents feedback inhibition. Bottom, synaptic interaction between PGN and TC neurons leads to repetitive TC bursts. **c**, Hybrid circuit reconstruction using nRt/PGN model cell, in guinea-pig LGNd slices where TC cells are initially synaptically isolated: effect of incrementing nRt/PGN-mediated GABA conductance. Calibration bars, 0.1 s, 20 mV, 0.35 nA.